

# FEEDBACK CONTROL OF THE KURAMOTO MODEL DEFINED ON UNIFORM GRAPHS I: DETERMINISTIC NATURAL FREQUENCIES

KAZUYUKI YAGASAKI

**ABSTRACT.** We study feedback control of the Kuramoto model with uniformly spaced natural frequencies defined on uniform graphs which may be complete, random dense or random sparse. The control objective is to drive all nodes to the same constant rotational motion. For the case of node number  $n \geq 3$ , we establish the existence of exactly  $2^n$  synchronized solutions in the controlled Kuramoto model (CKM) and their saddle-node and pitchfork bifurcations, and determine their stability. In particular, we show that only a solution converging to the desired motion in the limit of infinite feedback gain is stable and the others are unstable. Based on the previous results, it is shown that (i) the solution to which the stable synchronized solution in the CKM converge as  $n \rightarrow \infty$  is always asymptotically stable in the continuous limit (CL) if it exists, and (ii) the asymptotically stable solution of the CL captures the asymptotic behavior of the CKM when the node number is sufficiently large, even if the graphs are random dense or sparse. We demonstrate the theoretical results by numerical simulations for the CKM on complete simple, and uniform random dense and sparse graphs.

## 1. INTRODUCTION

**1.1. Kuramoto model defined on on graphs.** We consider the Kuramoto model (KM) [22, 23] with natural frequencies defined on graphs  $G_n$ ,  $n \in \mathbb{N}$ ,

$$\frac{d}{dt} u_i^n(t) = \omega_i^n + \frac{K}{n\alpha_n} \sum_{j=1}^n w_{ij}^n \sin(u_j^n(t) - u_i^n(t)), \quad i \in [n] := \{1, 2, \dots, n\}, \quad (1.1)$$

where  $n$  is the node number;  $u_i^n(t) \in \mathbb{S}^1 = \mathbb{R}/2\pi\mathbb{Z}$  and  $\omega_i^n$ , respectively, represent the phase and natural frequency of the oscillator at the node  $i \in [n]$ ;  $K > 0$  is a coupling constant; and  $\alpha_n$  is a scaling factor which is one if  $G_n$  is dense. Here  $G_n = \langle V(G_n), E(G_n), W(G_n) \rangle$ ,  $n \in \mathbb{N}$ , represent a sequence of weighted graphs, where  $V(G_n) = [n]$  and  $E(G_n)$  are the sets of nodes and edges, respectively, and  $W(G_n)$  is an  $n \times n$  weight matrix given by

$$(W(G_n))_{ij} = \begin{cases} w_{ij}^n & \text{if } (i, j) \in E(G_n); \\ 0 & \text{otherwise.} \end{cases}$$

---

*Date:* January 28, 2026.

*2020 Mathematics Subject Classification.* 34C15; 34H05; 45J05; 34D06; 34C23; 37G10; 34D20; 45M10; 05C90.

*Key words and phrases.* Kuramoto model; feedback control; continuum limit; synchronization; bifurcation; stability.

The edge set is expressed as

$$E(G_n) = \{(i, j) \in [n]^2 \mid (W(G_n))_{ij} \neq 0\},$$

where each edge is represented by an ordered pair of nodes  $(i, j)$ , which is also denoted by  $j \rightarrow i$ , and a loop is allowed. If  $W(G_n)$  is symmetric, then  $G_n$  represents an undirected weighted graph and each edge is also denoted by  $i \sim j$  instead of  $j \rightarrow i$ . When  $G_n$  is a simple graph,  $W(G_n)$  is a matrix whose elements are  $\{0, 1\}$ -valued. When  $G_n$  is a random graph,  $W(G_n)$  is a random matrix. We say that the graph  $G_n$  is *dense* if  $\#E(G_n)/(\#V(G_n))^2 > 0$  as  $n \rightarrow \infty$ , and that it is *sparse* if  $\#E(G_n)/(\#V(G_n))^2 \rightarrow 0$  as  $n \rightarrow \infty$ .

The weight matrix  $W(G_n)$  is given as follows: Let  $I = [0, 1]$  and let  $W \in L^2(I^2)$  be a measurable function. If  $G_n, n \in \mathbb{N}$ , are deterministic dense graphs, then

$$w_{ij}^n = \langle W \rangle_{ij}^n := n^2 \int_{I_i^n \times I_j^n} W(x, y) dx dy, \quad (1.2)$$

where

$$I_i^n := \begin{cases} [(i-1)/n, i/n] & \text{for } i < n; \\ [(n-1)/n, 1] & \text{for } i = n. \end{cases}$$

If  $G_n, n \in \mathbb{N}$ , are random dense graphs, then  $w_{ij}^n = 1$  with probability

$$\mathbb{P}(j \rightarrow i) = \langle W \rangle_{ij}^n, \quad (1.3)$$

where the range of  $W$  is contained in  $I$ . If  $G_n, n \in \mathbb{N}$ , are random sparse graphs, then  $w_{ij}^n = 1$  with probability

$$\mathbb{P}(j \rightarrow i) = \alpha_n \langle \tilde{W}_n \rangle_{ij}^n, \quad \tilde{W}(x, y) := \alpha_n^{-1} \wedge W(x, y), \quad (1.4)$$

where  $W$  is a nonnegative function,  $\alpha_n = n^{-\gamma}$  with  $\gamma \in (0, \frac{1}{2})$ , and  $a \wedge b = \min(a, b)$  for  $a, b \in \mathbb{R}$ . For the random cases, the graph  $G_n$  is a *Erdős-Rényi* model. In both cases, the connection probabilities are determined by a measurable function  $W(x, y)$  defined on  $I^2$ , which is usually called a *graphon* [26].

Such coupled oscillators on complex networks have recently attracted much attention and have been extensively studied. They provide many mathematical models in various fields such as physics, chemistry, biology, social sciences and engineering. Among them, the KM is one of the most representative models and has been generalized in several directions. It has very frequently been subject to research, especially to discuss the synchronization phenomenon. See [1, 2, 9, 33–35, 37] for the reviews of vast literature on coupled oscillators in complex networks including the KM and its generalizations. For the classical KM with uniformly spaced natural frequencies, all synchronized solutions and their stability were completely characterized in [40]. Related stability results for KMs on general coupling graphs can be found, for example, in [8, 16].

**1.2. Continuum limits and graphons.** In the previous work [19], coupled oscillator networks such as (1.1) were studied and shown to be well approximated by the corresponding continuum limits (CLs), for instance, which is given by

$$\frac{\partial}{\partial t} u(t, x) = \omega(x) + K \int_I W(x, y) \sin(u(t, y) - u(t, x)) dy, \quad x \in I, \quad (1.5)$$

for (1.1) if the natural frequencies  $\omega_i^n$ ,  $i \in [n]$ , are determined by the  $L^2$  function  $\omega(x)$  on  $I$  as

$$\omega_i^n = n \int_{I_i^n} \omega(x) dx, \quad i \in [n]. \quad (1.6)$$

We call  $\omega(x)$  a *frequency function* and assume that it is not a constant function. More general cases in which networks of coupled oscillators are defined on multiple graphs which may be deterministic dense, random dense or random sparse were discussed in [19]. Some results on the stability of solutions to the coupled oscillators and CLs were also refined in [40]. Similar results for such networks which are defined on single graphs and have the same natural frequency were obtained earlier in [20, 27, 28, 30] except for the stability of solutions although they are not applicable to (1.1) and (1.5).

Such a CL was introduced for the classical KM, which depends on a single complete simple graph but may have natural frequencies depending on each node, without a rigorous mathematical guarantee very early in [11], and fully discussed for the case of equally placed natural frequencies with any odd node number  $n \geq 3$  very recently in [40]. In particular, bifurcations and stability of synchronized solutions were proven to be very different between the classical KM and its CL. Moreover, bifurcations of completely synchronized solutions or twisted solutions in CLs for the KM of identical oscillators with two-mode interaction depending on two graphs or defined on nearest neighbor graphs with feedback control or not were discussed by the center manifold reduction technique [18], which is a standard one in dynamical systems theory [15, 38], in [41–43]. Similar CLs were also utilized for the KM with nonlocal coupling and a single or zero natural frequency in [14, 29, 31, 39].

**1.3. Related work on feedback control of coupled oscillators.** The control problem of coupled oscillator networks is important not only from a theoretical viewpoint but also for applications, and has attracted much attention [6, 10, 32]. Such studies are also significant in practice, since situations frequently arise in which all coupled oscillators are desired to exhibit the same rhythmic motion such as heart beats. In particular, for Kuramoto-type models, various control strategies have been proposed depending on the network structure and the form of control inputs.

For instance, coupled oscillator networks defined on multiple graphs have been studied from the viewpoint of control [12, 13, 19, 41]. In these works, additional coupling graphs are introduced to avoid undesired synchronization, which may otherwise lead to traffic congestion or collapse of networked systems. In particular, in [41], it was shown that synchronized solutions, which are intended to be avoided, can be unstable, and their stability and bifurcations were analyzed theoretically.

On the other hand, feedback control of synchronized states in the KM on deterministic dense, random dense and random sparse graphs has been studied numerically or theoretically in [19, 25, 36, 43, 45]. In these studies, a prescribed desired motion or position is incorporated into the dynamics as an external input, which is often periodic. Such a periodic input is referred to as a *pacemaker* in [25, 45]. However, the stability and bifurcations of the desired synchronized state were not clarified theoretically in [19, 25, 36, 45], although those of twisted solutions chosen as desired states were analyzed theoretically in [43].

**1.4. Object of the paper.** In this paper, we deal with the case of uniform graphs, i.e.,  $W(x, y) = p$ , which may be deterministic dense, random dense or random sparse. We attempt to control the KM (1.1) so that each node exhibits the desired motion  $V(t) = V_1 t + V_0$ , where  $V_1, V_0$  are constants, although more general desired motion can be treated similarly. So we add the control force  $b_1 \sin(V(t) - u_i^n(t)) + b_0$  to each node as

$$\begin{aligned} \frac{d}{dt} u_i^n(t) = & \omega_i^n + \frac{K}{n\alpha_n} \sum_{j=1}^n w_{ij}^n \sin(u_j^n(t) - u_i^n(t)) \\ & + b_1 \sin(V(t) - u_i^n(t)) + b_0, \quad i \in [n], \end{aligned} \quad (1.7)$$

where the constants  $b_1$  and  $b_0$  represent the feedback gain and stationary input, respectively. Here we include the stationary input  $b_0$  for simplicity of analysis. The corresponding CL is given by

$$\begin{aligned} \frac{\partial}{\partial t} u(t, x) = & \omega(x) + pK \int_I \sin(u(t, y) - u(t, x)) dy \\ & + b_1 \sin(V(t) - u(t, x)) + b_0. \end{aligned} \quad (1.8)$$

A restricted case was studied and some numerical simulation results were provided in [19]. We remark that the CL (1.8) is the same even if the graphs  $G_n$ ,  $n \in \mathbb{N}$ , are complete simple, random dense or random sparse.

We see that the CL (1.8) admits a particular solution

$$u(t, x) = U(x) + V(t), \quad U(x) = \arcsin\left(\frac{\omega(x) - V_1 + b_0}{pKC + b_1}\right), \quad (1.9)$$

where the constant  $C > 0$  satisfies

$$C = \int_I \sqrt{1 - \left(\frac{\omega(x) - V_1 + b_0}{pKC + b_1}\right)^2} dx, \quad (1.10)$$

if

$$b_0 = V_1 - \int_I \omega(x) dx \quad (1.11)$$

and

$$\sup_{x \in I} |\omega(x) - V_1 + b_0| \leq pKC + b_1. \quad (1.12)$$

In particular, the solution (1.9) is continuous in  $t$  and  $x$ . Moreover, when the graphs  $G_n$ ,  $n \in \mathbb{N}$ , are complete, i.e.,  $w_{ij}^n = p$ ,  $i, j \in [n]$ , the controlled Kuramoto model (CKM) (1.7) has a particular solution

$$u_i^n(t) = U_i^n + V(t), \quad U_i^n = \arcsin\left(\frac{\omega_i^n - V_1 + b_0}{pKC_D + b_1}\right), \quad (1.13)$$

where the constant  $C_D > 0$  satisfies

$$C_D = \frac{1}{n} \sum_{i=1}^n \sqrt{1 - \left(\frac{\omega_i^n - V_1 + b_0}{pKC_D + b_1}\right)^2} \quad (1.14)$$

if

$$b_0 = V_1 - \frac{1}{n} \sum_{i=1}^n \omega_i^n \quad (1.15)$$

and

$$\sup_{i \in [n]} |\omega_i^n - V_1 + b_0| \leq pK C_D + b_1. \quad (1.16)$$

See Appendix A for the derivation of (1.9) and (1.13). In particular, as  $b_1 \rightarrow \infty$ , the solutions (1.9) and (1.13), respectively, tend to

$$u(t, x) = V(t) \quad \text{and} \quad u_i^n(t) = V(t),$$

which coincide with the desired motions completely.

Specifically, we choose

$$\omega(x) = a(x - \frac{1}{2}), \quad (1.17)$$

where  $a > 0$  is a constant, as the frequency function as in [40], so that by (1.6)

$$\omega_i^n = \frac{a}{2n}(2i - n - 1), \quad i \in [n], \quad (1.18)$$

i.e., the natural frequencies are uniformly spaced. In addition, by (1.11) and (1.15)  $b_0 = V_1$ . We assume that the node number  $n \geq 3$ , and prove that for  $a, pK > 0$  fixed the solution (1.13) to the CKM (1.7) suffers a saddle-node bifurcation at some value of  $b_1$  where a pair of stable and unstable ones are born, and the solution (1.9) is always asymptotically stable in the CL (1.8) whenever it exists, as in the uncontrolled KM (1.1) and its CL (1.5) (see [40]). They are also proven to be the only synchronized solutions that are or can be stable in the CKM (1.7) and CL (1.8), respectively, when  $b_1 > 0$  and  $K > 0$  is small enough for them not to exist for  $b_1, b_0 = 0$ . Moreover, we show based on the results of [19, 40] that the solution (1.9) to the CL (1.8) behaves as it is an asymptotically stable one in the CKM (1.7) for  $n > 0$  sufficiently large, even if the graphs are random dense or sparse. In the companion paper [21], we discuss a similar control problem for the KM (1.1) with random natural frequencies.

**1.5. Outline of the paper.** The outline of this paper is as follows. In Section 2, we review fundamental theoretical results from [19] and [40] for coupled nonlinear oscillator networks in the context of (1.7) and (1.8). These results play an important role in the analysis in Sections 4 and 5. In Section 3, we present our main results on synchronized solutions of the CKM (1.7) on complete graphs. The CKM (1.7) is transformed into an equivalent autonomous system, all its equilibria, the number of which is exactly  $2^n$ , are characterized, and their bifurcations and stability are determined. In particular, we prove that the equilibrium corresponding to the solution (1.13) undergoes a saddle-node bifurcation, at which a pair of stable and unstable equilibria is created, while all other equilibria are unstable when  $b_1 > 0$  and  $K > 0$  is sufficiently small so that no equilibrium exists for  $b_1 = b_0 = 0$ . In Section 4, we analyze the CL (1.8) and show that the solution (1.9) is always asymptotically stable whenever it exists, whereas all other continuous and discontinuous synchronized solutions are unstable when  $b_1 > 0$  and  $K > 0$  is sufficiently small so that no synchronized solution exists for  $b_1 = b_0 = 0$ . In Section 5, we discuss the behavior of the CKM (1.7) on random dense and sparse graphs, using the results of Section 4 for the CL (1.8), based on the fundamental theory reviewed in Section 2. Finally, in Section 6, we illustrate the theoretical results by numerical simulations of the CKM (1.7) on complete simple graphs as well as on uniform random dense and sparse graphs.

## 2. PREVIOUS FUNDAMENTAL RESULTS

We review the fundamental theoretical results from [19, 40] in the context of (1.7) and (1.8). See Section 2 and Appendices A and B of [19] and Section 2 of [40] for more details including the proofs of the theorems stated below.

We begin with the initial value problem (IVP) of the CL (1.8). Let  $g(x) \in L^2(I)$  and let  $\mathbf{u} : \mathbb{R} \rightarrow L^2(I)$  stand for an  $L^2(I)$ -valued function on  $\mathbb{R}$ . We have the following from Theorem 2.1 of [19].

**Theorem 2.1.** *There exists a unique solution  $\mathbf{u}(t) \in C^1(\mathbb{R}; L^2(I))$  to the IVP of (1.8) with*

$$u(0, x) = g(x).$$

Moreover, the solution depends continuously on  $g$ .

We next consider the IVP of the CKM (1.7) and discuss the convergence of solutions in (1.7) to those in the CL (1.8). Since the right-hand side of (1.7) is Lipschitz continuous in  $u_i^n$ ,  $i \in [n]$ , we see by a fundamental result of ordinary differential equations (ODEs) (e.g., Theorem 2.1 of Chapter 1 of [7]) that the IVP of (1.7) has a unique solution. Given a solution  $u_n(t) = (u_1^n(t), u_2^n(t), \dots, u_n^n(t))$  to the IVP of the CKM (1.7), we define an  $L^2(I)$ -valued function  $\mathbf{u}_n : \mathbb{R} \rightarrow L^2(I)$  as

$$\mathbf{u}_n(t) = \sum_{i=1}^n u_i^n(t) \mathbf{1}_{I_i^n}, \quad (2.1)$$

where  $\mathbf{1}_{I_i^n}$  represents the characteristic function of  $I_i^n$  for  $i \in [n]$ . Let  $\|\cdot\|$  denote the norm in  $L^2(I)$ . We have the following from Theorem 2.3 of [19] (see also Theorem 2.2 of [40]).

**Theorem 2.2.** *If  $\mathbf{u}_n(t)$  is the solution to the IVP of the CKM (1.7) with the initial condition*

$$\lim_{n \rightarrow \infty} \|\mathbf{u}_n(0) - \mathbf{u}(0)\| = 0 \quad a.s.,$$

then for any  $\tau > 0$  we have

$$\lim_{n \rightarrow \infty} \max_{t \in [0, \tau]} \|\mathbf{u}_n(t) - \mathbf{u}(t)\| = 0 \quad a.s.,$$

where  $\mathbf{u}(t)$  represents the solution to the IVP of the CL (1.8).

We next discuss the stability of solutions to (1.7) and (1.8). We also obtain the following result, slightly modifying the proof of Theorem 2.5 in [19] (see also Theorem 2.3 of [40]).

**Theorem 2.3.** *Suppose that the CKM (1.7) and CL (1.8) have solutions  $\bar{\mathbf{u}}_n(t)$  and  $\bar{\mathbf{u}}(t)$ , respectively, such that*

$$\lim_{n \rightarrow \infty} \|\bar{\mathbf{u}}_n(t) - \bar{\mathbf{u}}(t)\| = 0 \quad a.s. \quad (2.2)$$

for any  $t \in [0, \infty)$ . Then the following hold:

- (i) *If for any  $\varepsilon > 0$ , there exist  $\delta_1 > 0$  such that for  $n > 0$  sufficiently large, any solution  $u_k^n(t)$ ,  $k \in [n]$ , to the CKM (1.7) with*

$$|u_k^n(0) - \bar{u}_k^n(0)| < \delta_1, \quad k \in [n],$$

*satisfies*

$$|u_k^n(t) - \bar{u}_k^n(t)| < \varepsilon, \quad k \in [n], \quad a.s.,$$

then  $\bar{\mathbf{u}}(t)$  is stable. Moreover, if for any  $\varepsilon > 0$ , there exists  $\delta_2 > 0$  such that for  $n > 0$  sufficiently large, any solution  $u_k^n(t)$ ,  $k \in [n]$ , to the CKM (1.7) with

$$|u_k^n(0) - \bar{u}_k^n(0)| < \delta_2, \quad k \in [n],$$

converges to  $\bar{\mathbf{u}}_n(t)$ ,  $k \in [n]$ , then  $\bar{\mathbf{u}}(t)$  is asymptotically stable.

- (ii) If  $\bar{\mathbf{u}}(t)$  is stable, then for any  $\varepsilon, T > 0$  there exists  $\delta > 0$  such that for  $n > 0$  sufficiently large, if  $\mathbf{u}_n(t)$  is a solution to the CKM (1.7) satisfying

$$\|\mathbf{u}_n(0) - \bar{\mathbf{u}}_n(0)\| < \delta,$$

then

$$\|\mathbf{u}_n(t) - \bar{\mathbf{u}}_n(t)\| < \varepsilon \quad a.s.$$

Moreover, if  $\bar{\mathbf{u}}(t)$  is asymptotically stable, then

$$\lim_{t \rightarrow \infty} \lim_{n \rightarrow \infty} \|\mathbf{u}_n(t) - \bar{\mathbf{u}}_n(t)\| = 0 \quad a.s.$$

**Remark 2.4.** In the definition of stability and asymptotic stability of solutions to the CL (1.8), we cannot distinguish two solutions that are different only in a set with the Lebesgue measure zero. See also Section 2 of [40].

Without assuming the existence of the solutions  $\bar{\mathbf{u}}_n(t)$  to the CKM (1.7) satisfying (2.2), we have the following result as a corollary of Theorem 2.3 (see Corollary 2.6 of [40]).

**Corollary 2.5.** Suppose that the CL (1.8) has a stable solution  $\bar{\mathbf{u}}(t)$ . Then for any  $\varepsilon, T > 0$  there exists  $\delta > 0$  such that for  $n > 0$  sufficiently large, if  $\mathbf{u}_n(t)$  is a solution to the KM (1.7) satisfying

$$\|\mathbf{u}_n(0) - \bar{\mathbf{u}}(0)\| < \delta,$$

then

$$\max_{t \in [0, T]} \|\mathbf{u}_n(t) - \bar{\mathbf{u}}(t)\| < \varepsilon \quad a.s.$$

Moreover, if  $\bar{\mathbf{u}}(t)$  is asymptotically stable, then

$$\lim_{t \rightarrow \infty} \lim_{n \rightarrow \infty} \|\mathbf{u}_n(t) - \bar{\mathbf{u}}(t)\| = 0 \quad a.s.$$

Corollary 2.5 implies that  $\bar{\mathbf{u}}(t)$  behaves as if it is an (asymptotically) stable solution in the CKM (1.7), when  $n > 0$  is sufficiently large. We have the following from Theorems 2.7 and 2.9 of [40].

**Theorem 2.6.** Suppose that the hypothesis of Theorem 2.3 holds. Then the following hold:

- (i) If  $\mathbf{u}_n(t)$  is unstable a.s. for  $n > 0$  sufficiently large and no stable solution to the CKM (1.7) converges to  $\mathbf{u}(t)$  a.s. as  $n \rightarrow \infty$ , then  $\mathbf{u}(t)$  is unstable;
- (ii) If  $\mathbf{u}(t)$  is unstable, then so is  $\mathbf{u}_n(t)$  for  $n > 0$  sufficiently large.

**Theorem 2.7.** If  $\bar{\mathbf{u}}(t)$  is unstable, then for any  $\varepsilon, \delta > 0$  there exist  $\tau, N > 0$  such that for  $n > N$

$$\|\mathbf{u}_n(\tau) - \bar{\mathbf{u}}(\tau)\| > \varepsilon, \quad a.s.$$

where  $\mathbf{u}_n(t)$  is a solution to the KM (1.7) satisfying

$$\|\mathbf{u}_n(0) - \bar{\mathbf{u}}(0)\| < \delta.$$

**Remark 2.8.**

- (i) *Only under the hypothesis of Theorem 2.6,  $\mathbf{u}(t)$  is not necessarily unstable even if  $\mathbf{u}_n(t)$  is unstable for  $n > 0$  sufficiently large. Moreover,  $\mathbf{u}(t)$  may be asymptotically stable even if  $\mathbf{u}_n(t)$  is unstable for  $n > 0$  sufficiently large. This behavior was proven to occur for the classical KM (1.1) on complete simple graphs and its CL (1.5) previously in [40]. We will see below that it also occurs for the CKM (1.7) on complete graphs and its CL (1.8).*
- (ii) *Theorem 2.7 implies that  $\bar{\mathbf{u}}(t)$  behaves as if it is an unstable solution in the CKM (1.7), when  $n > 0$  is sufficiently large.*

### 3. CONTROLLED KURAMOTO MODEL ON COMPLETE GRAPHS

In this section, we present our main results on synchronized solutions of the CKM (1.7) with the uniformly spaced natural frequencies (1.18) on complete graphs, i.e.,  $w_{ij} = p \in (0, 1]$ ,  $i, j \in [n]$ , and  $\alpha_n = 1$ . We transform the CKM (1.7) into a tractable autonomous system, detect all its equilibria, the number of which is exactly  $2^n$ , and determine their bifurcation structure and stability. A key result of this section is that the equilibrium corresponding to the synchronized solution (1.13) undergoes a saddle-node bifurcation, at which a pair of stable and unstable equilibria are born. Moreover, we prove that, when  $b_1 > 0$  and  $K > 0$  is sufficiently small, all other equilibria are unstable, and no equilibrium exists for  $b_1 = b_0 = 0$ . These results provide a complete picture of synchronization, bifurcations and stability for the CKM (1.7) on complete graphs.

Throughout this section, we take any integer  $n \geq 3$  as the node number. Let

$$v_i = u_i^n - V(t), \quad i \in [n]. \quad (3.1)$$

Since we take  $b_0 = V_1$ , Eq. (1.7) becomes

$$\dot{v}_i = (2i - n - 1)\nu + \frac{pK}{n} \sum_{j=1}^n \sin(v_j - v_i) - b_1 \sin v_i, \quad i \in [n], \quad (3.2)$$

where  $\nu = a/2n$ . If Eq. (3.2) has an equilibrium at  $v_i = \zeta_i$ ,  $i \in [n]$ , then

$$u_i^n = \zeta_i + V(t), \quad i \in [n]. \quad (3.3)$$

is a solution to the CKM (1.7). Let  $v = (v_1, \dots, v_n)$  and  $\zeta = (\zeta_1, \dots, \zeta_n)$ . If the equilibrium  $v = \zeta$  is (asymptotically) stable, then so is the solution (3.3), and if a bifurcation of  $v = \zeta$  occurs, then so does that of (3.3). Hence, we analyze the system (3.2) instead of the CKM (1.7) below. Our approaches are modifications of ones used in [40], in which the classical KM given by (1.1) with  $p = 1$  was analyzed when  $n$  is any odd number with  $n \geq 3$ , although the modifications are not straightforward.

**3.1. Equilibria.** Let  $\sigma = \{\sigma_i\}_{i=1}^n$  be a sequence of length  $n$  with  $\sigma_i \in \{-1, 1\}$ ,  $i \in [n]$ , and let

$$\Sigma_n = \{\sigma = \{\sigma_i\}_{i=1}^n \mid \sigma_i \in \{-1, 1\}, i \in [n]\}.$$

For each  $\sigma \in \Sigma_n$ , we define  $C_D^\sigma$  such that

$$C_D^\sigma = \frac{1}{n} \sum_{i=1}^n \sigma_i \sqrt{1 - \left( \frac{(2i - n - 1)\nu}{pK C_D^\sigma + b_1} \right)^2}, \quad (3.4)$$

and write

$$v_i^\sigma = \begin{cases} \phi_i & \text{if } \sigma_i = 1; \\ \pi - \phi_i & \text{if } \sigma_i = -1 \text{ and } \phi_i \geq 0; \\ -\phi_i - \pi & \text{if } \sigma_i = -1 \text{ and } \phi_i < 0, \end{cases} \quad (3.5)$$

where

$$\phi_i = \arcsin \left( \frac{(2i - n - 1)\nu}{pK C_D^\sigma + b_1} \right). \quad (3.6)$$

As in Theorem 4.1 of [40], we can prove the following on the existence of equilibria in (3.2).

**Theorem 3.1.**

- (i) For each  $\sigma \in \Sigma_n$ ,  $v = v^\sigma \in \mathbb{T}^n := \prod_{i=1}^n \mathbb{S}^1$  gives an equilibrium in (3.2), when  $C_D^\sigma$  satisfies (3.4). Moreover, no other equilibrium exists in (3.2) for  $b_1 \neq 0$ .
- (ii) Fix  $b_1, a, pK > 0$  and let  $i \leq n/2$ . If the equilibrium  $v = v^\sigma$  with  $\sigma_i = -1$  and  $\sigma_{n-i+1} = 1$  exists, then so does  $v = v^{\bar{\sigma}}$  with  $\bar{\sigma}_i = 1$ ,  $\bar{\sigma}_{n-i+1} = -1$  and  $\bar{\sigma}_j = \sigma_j$ ,  $j \in [n] \setminus \{i, n-i+1\}$ , and vice versa.

*Proof.* Let  $\zeta = (\zeta_1, \dots, \zeta_n)$  denote an equilibrium of (3.2). Recall that  $b_0 = V_1$ . We begin with the following lemma.

**Lemma 3.2.** *We have*

$$\sum_{i=1}^n \sin \zeta_i = 0.$$

*Proof.* Since the right-hand sides of (3.2) are zero when  $v_i = \zeta_i$ ,  $i \in [n]$ , we sum up them to obtain the desired result.  $\square$

Let

$$C_\zeta = \frac{1}{n} \sum_{i=1}^n \cos \zeta_i.$$

Using Lemma 3.2 and (3.2), we have

$$(2i - n - 1)\nu - (pK C_\zeta + b_1) \sin \zeta_i = 0. \quad (3.7)$$

Hence, if  $\phi_i \geq 0$  (resp.  $\phi_i < 0$ ), then  $\zeta_i = \phi_i$  or  $\pi - \phi_i$  (resp.  $\zeta_i = \phi_i$  or  $-\pi - \phi_i$ ),  $i \in [n]$ , where  $\phi_i$  is given by (3.6) with  $C_D^\sigma = C_\zeta$ . This yields part (i). By (3.4), we have  $C_D^\sigma = C_D^{\bar{\sigma}}$ , so that  $\phi_i^\sigma = \phi_i^{\bar{\sigma}}$ ,  $i \in [n]$ . Hence, we obtain part (ii).  $\square$

For  $\sigma \in \Sigma_n$ , we define

$$\chi^\sigma(\xi) = \frac{1}{n} \sum_{i=1}^n \sigma_i \sqrt{1 - \left( \frac{2i - n - 1}{n - 1} \xi \right)^2},$$

where  $\xi \in [0, 1]$ . Letting  $\xi = (n - 1)\nu / |pK C_D^\sigma + b_1|$ , we rewrite (3.4) as

$$\frac{pK}{b_1} = \bar{\chi}^\sigma(\xi) := \frac{\xi}{\pm \beta - \xi \chi^\sigma(\xi)}, \quad \beta = \frac{(n - 1)\nu}{pK} > 0, \quad (3.8)$$

where the upper or lower is taken, depending on whether  $pK \chi^\sigma(\xi) + b_1$  is positive or negative. From Theorem 3.1(i) we immediately obtain the following corollary.

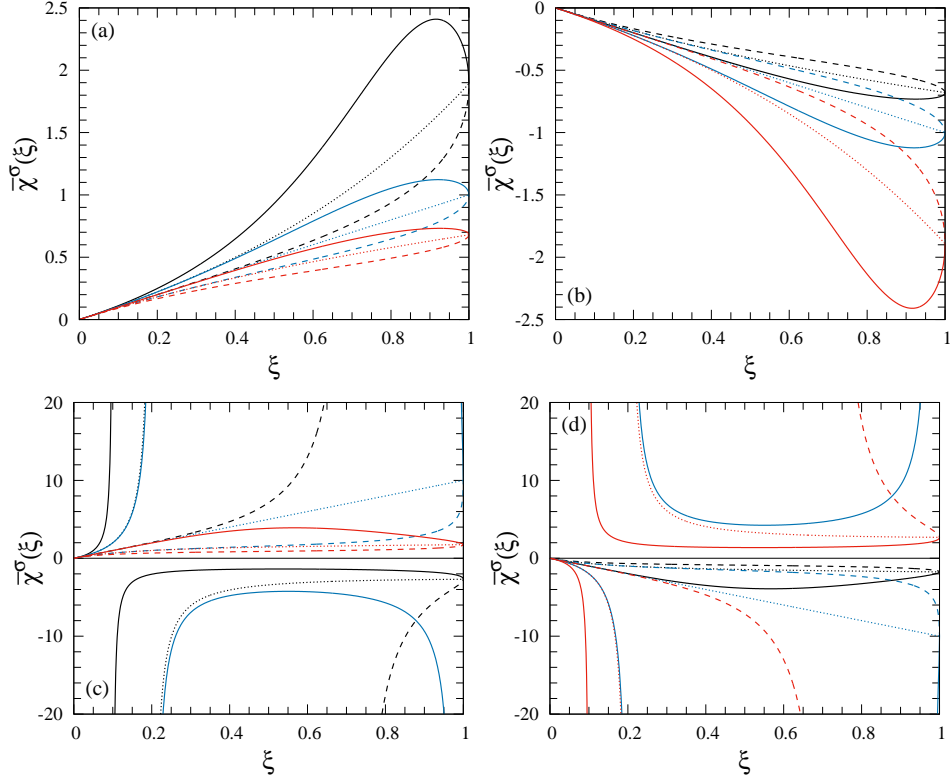


FIGURE 1. Function  $\bar{\chi}^\sigma(\xi)$  for  $n = 4$ : (a) and (b)  $\beta = 1$ ; (c) and (d) 0.1. In plates (a) and (c) (resp. plates (b) and (d)) the sign ‘+’ (resp. ‘-’) is taken in (3.8). See the text for more details.

**Corollary 3.3.** *Fix the value of  $pK > 0$ . If  $\xi \in (0, 1]$  satisfies (3.8) for  $\sigma \in \Sigma_n$  and  $b_1 > 0$ , then  $v^\sigma$  given by (3.5) with*

$$\phi_i = \pm \arcsin \left( \frac{2i - n - 1}{n - 1} \xi \right),$$

*instead of (3.6), is an equilibrium in (3.2), where the upper or lower is taken, depending on whether  $pK\chi^\sigma(\xi) + b_1$  is positive or negative.*

**Remark 3.4.**

- (i) *From Theorem 3.1 we easily see that the number of equilibria in (3.2), which correspond to synchronized solutions of the form (1.7), is exactly  $2^n$ .*
- (ii) *It is clear that  $v^\sigma \neq v^{\hat{\sigma}}$  if  $\sigma \neq \hat{\sigma}$ ,  $\xi \neq 1$  and  $b_1 \neq 0$ .*
- (iii) *From the result of [19, 40] we see that if  $b_1 = 0$ , then there exists a one-parameter family of equilibria in (3.2).*

The graph of  $\bar{\chi}^\sigma(\xi)$  is displayed for  $n = 4$  in Fig. 1. It is plotted as a solid line if  $\bar{\chi}^\sigma(\xi)$  has a local maximum or minimum, and as a dotted or dashed line otherwise, depending on whether  $\sigma_1 \neq \sigma_n$  or not. The black and red lines represent the graph for  $(\sigma_2, \sigma_3) = (1, 1)$  and  $(-1, -1)$ , respectively, while the blue line for

$(\sigma_2, \sigma_3) = (1, -1)$  or  $(-1, 1)$ . We see that  $\bar{\chi}^\sigma(\xi)$  is bounded if  $\beta > 0$  is sufficiently large and that it is unbounded if  $\beta > 0$  is sufficiently small. We prove the following.

**Proposition 3.5.** *Suppose that*

$$\beta = \frac{(n-1)\nu}{pK} > \max_{\xi \in [0,1]} \xi \chi^\sigma(\xi) \quad \text{with } \sigma_i = 1, i \in [n]. \quad (3.9)$$

*Then the system (3.2) has no equilibrium when  $b_1 = 0$ .*

*Proof.* Assume that the hypothesis of the proposition holds. Then for any  $\sigma \in \Sigma_n$

$$\beta > \max_{\xi \in [0,1]} |\xi \chi^\sigma(\xi)|, \quad (3.10)$$

so that  $\bar{\chi}^\sigma(\xi)$  is bounded on  $[0, 1]$ . This implies the desired result since the relation (3.8) does not hold near  $b_1 = 0$ .  $\square$

**3.2. Bifurcations.** We next discuss bifurcations of the equilibria in (3.2) detected by Theorem 3.1 and equivalently by Corollary 3.3. The relation (3.8) gives a branch of equilibria when  $b_1$  is taken as a control parameter. As in Theorem 5.1 of [40], we prove the following on their bifurcations.

**Theorem 3.6.** *Fix the values of  $a, pK > 0$  and choose  $b_1$  as a control parameter. Then the following hold.*

- (i) *The equilibrium  $v^\sigma$  suffers a supercritical (resp. subcritical) saddle-node bifurcation at*

$$b_1 = \frac{pK}{\bar{\chi}^\sigma(\xi_0)} \quad (3.11)$$

*in (3.2) if and only if  $\bar{\chi}^\sigma(\xi)$  has a local maximum (resp. minimum) at  $\xi = \xi_0$  on  $(0, 1)$ . In particular, if  $\bar{\chi}^\sigma(\xi)$  is bounded on  $[0, 1]$  and*

$$\sigma_1, \sigma_n = 1, \quad \bar{\chi}^\sigma(1) \geq 0 \quad (\text{resp. } \sigma_1, \sigma_n = -1, \quad \bar{\chi}^\sigma(1) \leq 0), \quad (3.12)$$

*then a supercritical (resp. subcritical) saddle-node bifurcation occurs. Moreover, if  $b_1 > 0$ ,  $\sigma_i = 1, i \in [n]$ , and condition (3.9) holds, then  $\bar{\chi}^\sigma(\xi)$  has a unique local maximum and no local minimum, and  $v^\sigma$  suffers only one saddle-node bifurcation.*

- (ii) *Let  $v^{\sigma^{\pm\pm}}$  be four equilibria in (3.2) such that*

$$\sigma_i^{++} = \sigma_i^{--} = \sigma_i^{+-} = \sigma_i^{-+}, \quad i \neq 1, n,$$

*and*

$$\sigma_1^{++}, \sigma_1^{+-} = 1, \quad \sigma_1^{-+}, \sigma_1^{--} = -1, \quad \sigma_n^{++}, \sigma_n^{-+} = 1, \quad \sigma_n^{+-}, \sigma_n^{--} = -1.$$

*If  $\bar{\chi}^\sigma(1) \neq 0$ , then a pitchfork bifurcation where  $v^{\sigma^{++}}$  changes to  $v^{\sigma^{--}}$  and where  $v^{\sigma^{+-}}$  and  $v^{\sigma^{-+}}$  are born occurs at*

$$b_1 = \frac{pK}{\bar{\chi}^\sigma(1)}, \quad (3.13)$$

*where any of  $\sigma^{\pm\pm}$  may be chosen as  $\sigma$ . Moreover, the bifurcation is super- or subcritical if*

$$\frac{d\bar{\chi}^\sigma}{d\xi}(1) \quad \text{with } \sigma = \sigma^{+-} \text{ and } \sigma^{-+} \quad (3.14)$$

*is positive or negative, where any of  $\sigma^{+-}$  and  $\sigma^{-+}$  may be chosen as  $\sigma$ .*

*Proof.* We first easily see via Corollary 3.3 that if  $\xi \in (0, 1)$  satisfies (3.8), then  $v^\sigma$  is an equilibrium in (3.2). Hence, if  $\bar{\chi}^\sigma(\xi)$  has a local maximum (resp. minimum) at  $\xi = \xi_0$  on  $(0, 1)$ , then no value of  $\xi$  satisfies (3.8) for values of  $b_1$  that are smaller (resp. larger) than and close to (3.11) but two values of  $\xi$  satisfy it for values of  $b_1$  that are larger (resp. smaller) than and close to (3.11), so that the equilibrium  $v^\sigma$  suffers a supercritical (resp. subcritical) saddle-node bifurcation there. If  $\bar{\chi}^\sigma(\xi)$  is bounded on  $[0, 1]$  and condition (3.12) holds, then  $\bar{\chi}^\sigma(\xi)$  has a local maximum (resp. minimum), since  $\bar{\chi}^\sigma(0) = 0$  and

$$\frac{d\bar{\chi}^\sigma}{d\xi}(\xi) = \frac{\pm\beta + \xi^2 \frac{d\chi^\sigma}{d\xi}(\xi)}{(\pm\beta - \xi\chi^\sigma(\xi))^2} \rightarrow -\infty \quad (\text{resp. } +\infty) \quad (3.15)$$

as  $\xi \rightarrow 1$ . Note that

$$\begin{aligned} & \frac{d\chi^\sigma}{d\xi}(\xi) \\ &= -\frac{1}{n} \sum_{i=1}^n \sigma_i \left( \frac{2i-n-1}{n-1} \right)^2 \xi \left/ \sqrt{1 - \left( \frac{2i-n-1}{n-1} \right)^2 \xi^2} \right. \rightarrow -\infty \quad (\text{resp. } +\infty) \end{aligned}$$

as  $\xi \rightarrow 1$  under the conditions.

Assume that  $b_1 > 0$ ,  $\sigma_i = 1$ ,  $i \in [n]$ , and condition (3.9) holds. Since  $pK\chi^\sigma(\xi) + b_1 > 0$ , we have

$$\bar{\chi}^\sigma(\xi) = \frac{\xi}{\beta - \xi\chi^\sigma(\xi)} > 0$$

and

$$\frac{d\bar{\chi}^\sigma}{d\xi}(\xi) = \frac{\beta - \frac{\xi}{n} \sum_{i=1}^n \left( \frac{2i-n-1}{n-1} \right)^2 \xi \left/ \sqrt{1 - \left( \frac{2i-n-1}{n-1} \right)^2 \xi^2} \right.}{(\beta - \xi\chi^\sigma(\xi))^2}. \quad (3.16)$$

The numerator in (3.16) is monotonically decreasing on  $(0, 1)$  and positive at  $\xi = 0$  and goes to  $-\infty$  as  $\xi \rightarrow 1$  while the denominator is always positive. Hence,  $\bar{\chi}^\sigma(\xi)$  has a unique local maximum at which its derivative has a unique zero, and it has no local minimum. Thus, we obtain part (i).

On the other hand, assume that  $\bar{\chi}^\sigma(1) \neq 0$ . Then at  $\xi = 1$ , the four equilibria  $v^{\sigma^{\pm\pm}}$  coincide and the corresponding functions  $\bar{\chi}^{\sigma^{\pm\pm}}(\xi)$  have the same value. We see that  $\sigma^{++}$  and  $\sigma^{--}$ , respectively, satisfy the first and second equations of (3.15) as  $\xi \rightarrow 1$ , and that  $v^{\sigma^{+-}}$  and  $v^{\sigma^{-+}}$  exist in a pair by Theorem 3.1(ii) for values of  $b_1$  that are larger or smaller than and close to (3.13), depending on whether the quantity (3.14), which takes the same value for both of  $\sigma = \sigma^{+-}$  and  $\sigma^{-+}$ , is positive or negative. So we obtain part (ii).  $\square$

From Theorem 3.6 we can also estimate the numbers of saddle-node and pitchfork bifurcations if condition (3.9) holds, as in Remark 5.2 and Proposition 5.3 of [40].

**Proposition 3.7.** *Suppose that condition (3.9) holds. Then both the numbers of saddle-node and pitchfork bifurcations are at least  $2^{n-2}$ .*

*Proof.* We assume that condition (3.9) holds. From the proof of Proposition 3.5 we see that  $|\bar{\chi}^\sigma(\xi)|$  is bounded on  $[0, 1]$  as well as  $\bar{\chi}^\sigma(1) \neq 0$  for any  $\sigma \in \Sigma_n$ . Hence, the number of  $\sigma \in \Sigma_n$  satisfying condition (3.12) is  $2^{n-2}$ , so that by Theorem 3.6(i),

$2^{n-2}$  saddle-node bifurcations occur. Moreover, it follows from Theorem 3.6(ii) that  $2^{n-2}$  pitchfork bifurcations occur since  $\bar{\chi}^\sigma(1) \neq 0$  for any  $\sigma \in \Sigma_n$ .  $\square$

As in Proposition 4.4 of [40], we also have the following.

**Proposition 3.8.** *For any  $\sigma \in \Sigma_n$ , the equilibrium  $v^\sigma$  suffers no Hopf bifurcation.*

*Proof.* We compute each element of the Jacobian matrix  $A$  for the vector field of (3.2) as

$$A_{ij} = \begin{cases} -\frac{pK}{n} \sum_{j=1, j \neq i}^n \cos(v_j - v_i) - b_1 \cos v_i & \text{if } i = j; \\ \frac{pK}{n} \cos(v_j - v_i) & \text{if } i \neq j. \end{cases} \quad (3.17)$$

Thus, the matrix  $A$  is a symmetric and consequently has only real eigenvalues. This implies the desired result.  $\square$

**Remark 3.9.** *From Remark 3.4(ii) and Proposition 3.8 we see that no other bifurcation than ones detected in Theorem 3.6 occurs for equilibria in the system (3.2) if  $b_1 \neq 0$ .*

**3.3. Stability.** We now discuss the stability of the equilibria detected by Theorem 3.1 and equivalently by Corollary 3.3 in (3.2). As in Theorem 6.1 of [40], we prove the following on their stability.

**Theorem 3.10.** *Suppose that  $b_1 > 0$  and condition (3.9) holds. Then the following hold:*

- (i) *The equilibrium  $v^\sigma$  with  $\sigma_i = 1$  for all  $i \in [n]$  is asymptotically stable if  $\xi < \xi_0$  and unstable if  $\xi > \xi_0$ , where  $\xi_0$  is the unique local maximum of  $\bar{\chi}^\sigma(\xi)$  detected in Theorem 3.6(i).*
- (ii) *The equilibrium  $v^\sigma$  is unstable if  $\sigma_i = -1$  for some  $i \in [n]$ .*

*Proof.* Suppose that the hypotheses of the theorem hold. Fix  $\sigma \in \Sigma_n$  and increase  $\xi \in (0, 1)$  along a branch of equilibria,  $v^\sigma$  with  $\bar{\chi}^\sigma(\xi)$ . We write  $v^\sigma(\xi) = v^\sigma \in \mathbb{T}^n$  and  $f(v; b_1)$  for the vector field of (3.2). By Proposition 3.5 the branch  $b_1 = pK/\bar{\chi}^\sigma(\xi)$  does not intersect  $b_1 = 0$ . We begin with the following lemma.

**Lemma 3.11.** *Suppose that the multiplicity of the zero eigenvalue of the Jacobian matrix  $D_v f(v^\sigma(\xi); b_1)$  with  $\bar{\chi}^\sigma(\xi)$ ,  $\sigma \in \Sigma_n$ , changes at  $\xi = \xi_*$  when  $\xi$  increases on  $(0, 1)$ . Then  $\bar{\chi}^\sigma(\xi)$  has an extremum at  $\xi = \xi_*$  and the change of the multiplicity is one at most.*

*Proof.* We apply arguments similar to those used in the proof of Lemma 6.2 of [40].

Since  $D_v f(v^\sigma(\xi); b_1)$  is symmetric, its eigenvalues are real and geometrically simple, as shown in the proof of Proposition 3.8. In particular, if the eigenvalues change their signs, then they must become zero.

Assume that  $D_v f(v^\sigma(\xi); b_1)$  has a simple zero eigenvalue when Eq. (3.8) holds with  $\xi = \xi_* \in (0, 1)$ . Let  $\bar{e} \in \mathbb{R}^n$  denote the associated eigenvector. Then the equilibrium  $v^\sigma(\xi_*)$  has a one-dimensional center manifold [15, 24, 38] on which the system (3.2) reduces to

$$\dot{v}_c = c_1 v_c^j + \cdots + c_2 (b_1 - b_{1*}) + \cdots, \quad v_c \in \mathbb{R}, \quad (3.18)$$

where  $b_{1*} = pK/\bar{\chi}^\sigma(\xi_*)$ ,  $c_1, c_2 \in \mathbb{R}$  are constants and  $j > 1$  is an even integer, since the eigenvalue does not change its sign if  $j$  is odd. If  $\bar{e}$  is linearly independent of

$(dv^\sigma/d\xi)(\xi_*)$ , then there exists a different equilibrium from  $v^\sigma(\xi)$  close to  $\xi = \xi_*$ , but coincide with it at  $\xi = \xi_*$ . This contradicts that the equilibrium  $v^\sigma(\xi_*)$  is isolated for  $\xi \in (0, 1)$  by Remark 3.4(ii). Hence, we can take  $\bar{e} = (dv^\sigma/d\xi)(\xi_*)$ , so that by (3.8)

$$\frac{d\bar{\chi}^\sigma}{d\xi}(\xi_*) = 0$$

since

$$\frac{\partial f}{\partial b_1}(v^\sigma(\xi_*); b_{1*}) = -(\sin v_1^\sigma(\xi_*), \dots, \sin v_n^\sigma(\xi_*))^T \neq 0$$

and by  $f(v^\sigma(\xi); pK/\bar{\chi}^\sigma(\xi)) \equiv 0$ ,

$$\begin{aligned} & \left. \frac{d}{d\xi} f\left(v^\sigma(\xi); \frac{pK}{\bar{\chi}^\sigma(\xi)}\right) \right|_{\xi=\xi_*} \\ &= D_v f(v^\sigma(\xi_*); b_{1*}) \frac{dv^\sigma}{d\xi}(\xi_*) - \frac{\partial f}{\partial b_1}(v^\sigma(\xi_*); b_{1*}) \frac{pK}{(\bar{\chi}^\sigma(\xi_*))^2} \frac{d\bar{\chi}^\sigma}{d\xi}(\xi_*) = 0, \end{aligned}$$

where the superscript ‘T’ represents the transpose operator. Similarly, we can show that  $D_v f(v^\sigma(\xi); b_1)$  never has a non-simple zero eigenvalue even when  $(d\bar{\chi}^\sigma/d\xi) = 0$ , since the equilibrium  $v^\sigma(\xi)$  is isolated for  $\xi \in (0, 1)$ . Thus, we obtain the desired result.  $\square$

We return to the proof of Theorem 3.10. Taking the limit  $\xi = (n-1)\nu/|pKC_D^\sigma + b_1| \rightarrow 0$ , we have  $b_1 \rightarrow +\infty$  and  $\phi_i \rightarrow 0$  in (3.6), so that by (3.5)

$$v_i^\sigma \rightarrow \begin{cases} 0 & \text{if } \sigma_i = 1; \\ \pi \text{ or } -\pi & \text{if } \sigma_i = -1, \end{cases}$$

since the branch  $b_1 = pK/\bar{\chi}^\sigma(\xi)$  does not intersect  $b_1 = 0$ . Let  $n_+$  and  $n_-$  be, respectively, the numbers of  $\sigma_i = 1$  and  $-1$ ,  $i \in [n]$ . The Jacobian matrix  $A = D_v f(v^\sigma(\xi); b_1)$  is written as

$$A = b_1 A_0 + O(1), \quad b_1 \rightarrow \infty,$$

as  $\xi \rightarrow 0$ , where  $A_0$  is an  $n \times n$  diagonal matrix whose  $n_-$  and  $n_+$  diagonal elements are 1 and  $-1$ , respectively. We immediately obtain the following.

**Lemma 3.12.** *Let  $\xi > 0$  be sufficiently small. Then the numbers of positive and negative eigenvalues of the matrix  $A$  are  $n_-$  and  $n_+$ , respectively. In particular, the matrix  $A$  has no positive eigenvalue if and only if  $n_+ = n$ , i.e.,  $n_- = 0$ .*

Let  $\sigma_i = 1$ ,  $i \in [n]$ , i.e.,  $n_- = 0$ . Since by Theorem 3.6(i)  $\bar{\chi}^\sigma(\xi)$  has an extremum only at  $\xi = \xi_0$ , it follows from Lemma 3.11 that only one eigenvalue of  $D_v f(v; b_1)$  with  $b_1 = pK/\bar{\chi}^\sigma(\xi)$  changes its sign once at  $\xi = \xi_0$  when  $\xi$  increases from zero to one. Noting that all of its eigenvalues are negative near  $\xi = 0$  by Lemma 3.12, we obtain part (i).

We turn to the proof of part (ii). We compute

$$\frac{dv_i^\sigma}{d\xi}(\xi) = \pm \sigma_i \left( \frac{2i-n-1}{n-1} \right) / \sqrt{1 - \left( \frac{2i-n-1}{n-1} \xi \right)^2}$$

and

$$\frac{\partial f_i}{\partial b_1}(v^\sigma(\xi); b_1) = \mp \sigma_i \left( \frac{2i-n-1}{n-1} \xi \right)$$

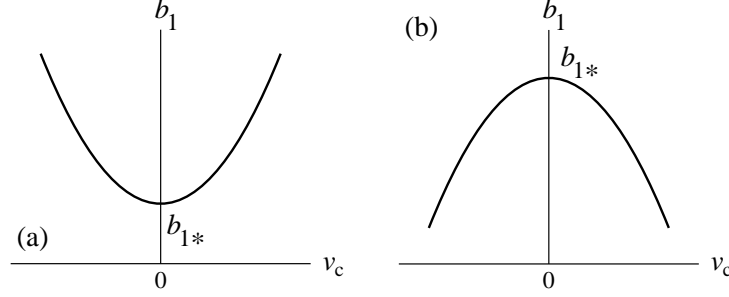


FIGURE 2. Bifurcation diagrams of equilibria in (3.18): (a)  $c_1/c_2 < 0$ ; (b)  $c_1/c_2 > 0$ .

for  $i \in [n]$  when  $b_1 = pK/\bar{\chi}^\sigma(\xi)$ , where  $f_i(v; b_1)$  is the  $i$ th element of  $f(v; b_1)$  and the upper or lower sign is taken simultaneously, depending on whether  $pK\bar{\chi}^\sigma(\xi) + b_1$  is positive or not.

Suppose that  $(d\bar{\chi}^\sigma/d\xi)(\xi)$  has a zero at  $\xi = \xi_*$  and let  $b_{1*} = pK/\bar{\chi}^\sigma(\xi_*) > 0$  be bounded. Then the Jacobian matrix  $D_v f(v^\sigma(\xi_*); b_{1*})$  has a simple zero eigenvalue and  $(dv/d\xi)(\xi_*)$  is the associated eigenvector. The equilibrium  $v^\sigma(\xi_*)$  has a one-dimensional center manifold on which the system (3.2) reduces to (3.18). See the proof of Lemma 3.11. In addition,  $c_1/c_2$  is negative or positive, whether  $\bar{\chi}^\sigma(\xi)$  has a local maximum or minimum at  $\xi = \xi_*$ , since by Theorem 3.6(i) a supercritical or subcritical saddle-node bifurcation occurs. See Fig. 2. Moreover, substituting  $v = (dv^\sigma/d\xi)(\xi_*)v_c + v^\sigma(\xi_*)$  into (3.2) and taking the inner product of the resulting equation with  $(dv/d\xi)(\xi_*)$ , we have

$$c_2 = \frac{dv_i^\sigma}{d\xi}(\xi_*) \cdot \frac{\partial f_i}{\partial b_1}(v^\sigma(\xi_*); b_{1*}) \bigg/ \left| \frac{dv_i^\sigma}{d\xi}(\xi_*) \right|^2 < 0$$

where the dot “ $\cdot$ ” represents the standard inner product, since

$$\frac{dv_i^\sigma}{d\xi}(\xi_*) \cdot \frac{\partial f_i}{\partial b_1}(v^\sigma(\xi_*); b_{1*}) = - \sum_{i=1}^{n_0} \left( \frac{2i-n-1}{n-1} \right)^2 \bigg/ \sqrt{1 - \left( \frac{2i-n-1}{n-1} \xi \right)^2} < 0.$$

We have

$$v_c = \frac{dv^\sigma}{d\xi}(\xi_*) \cdot (v - v^\sigma(\xi_*)) \bigg/ \left| \frac{dv^\sigma}{d\xi}(\xi_*) \right|^2,$$

so that  $v_c$  is negative or positive for  $v = v^\sigma(\xi)$  near  $\xi = \xi_*$ , depending on whether  $\xi$  is less or larger than  $\xi_*$ . Hence, we see via (3.18) that a negative (resp. positive) eigenvalue of  $D_v f(v^\sigma(\xi); b_1)$  with  $b_1 = pK/\bar{\chi}^\sigma(\xi)$  becomes positive (resp. negative) when  $\bar{\chi}^\sigma(\xi)$  has a local maximum (resp. minimum) at  $\xi = \xi_*$ , i.e.,  $c_1 > 0$  (resp.  $c_1 < 0$ ). See Fig. 2.

Fix  $\sigma \in \Sigma_n$  and change  $\xi$  from 0 to 1. We see that  $\bar{\chi}^\sigma(\xi)$  must take a local maximum before taking a local minimum since it does not become zero on  $(0, 1]$  by (3.10). Hence, if  $\sigma_i = -1$  for some  $i \in [n]$ , then  $v^\sigma(\xi)$  continues to be unstable when changing  $\xi$  from 0 to 1, since the number of positive eigenvalues of  $D_v f(v^\sigma(\xi); b_1)$  does not vanish. Thus, we obtain the desired result.  $\square$

**Remark 3.13.** *From the proof of Theorem 3.10 we see that the equilibrium  $v^\sigma$  with  $\sigma_i = -1$ ,  $i \in [n]$ , is stable for  $b_1 < 0$  with  $|b_1| \gg 1$ .*

By the relation (3.1) we have

$$u_i^n = v_i^\sigma + V(t) \quad (3.19)$$

as a synchronized solution in the CKM (1.7) for each  $\sigma \in \Sigma_n$ . In particular, when  $\sigma_i = 1$ ,  $i \in [n]$ , we have

$$u_i^n = \arcsin\left(\frac{2i-n-1}{n-1}\xi\right) + V(t), \quad \xi = \frac{(n-1)\nu}{pKC_D^\sigma + b_1},$$

which coincides with (1.13). The synchronized solution (3.19) suffers such bifurcations as detected in Theorem 3.6 and has the same stability type as the equilibrium  $v^\sigma$  in (3.2), which is determined in Theorem 3.10. In particular, it is stable for  $\xi < \xi_*$  and unstable for  $\xi > \xi_*$  if  $\sigma_i = 1$  for  $i \in [n]$ , and always unstable if  $\sigma_i = -1$  for some  $i \in [n]$ , under the hypotheses of Theorem 3.10.

#### 4. CONTINUUM LIMITS

In Section 3, we obtained a complete description of equilibria in the CKM (1.7) with the natural frequencies (1.18) on complete graphs, including their bifurcation structure and stability. In this section, based on the fundamental results in Section 2 and the characterization of equilibria and their stability, we study continuous and discontinuous solutions and their stability in the CL (1.8) with the frequency function (1.17). A similar approach was utilized in [40].

The synchronized continuous solution (1.9) becomes

$$u(t, x) = U(x) + V(t), \quad U(x) = \arcsin\left(\frac{a(x - \frac{1}{2})}{pKC + b_1}\right), \quad (4.1)$$

where the constant  $C > 0$  satisfies

$$C = \frac{pKC + b_1}{a} \left( \arcsin\left(\frac{a}{2(pKC + b_1)}\right) + \frac{a}{2(pKC + b_1)} \sqrt{1 - \left(\frac{a}{2(pKC + b_1)}\right)^2} \right), \quad (4.2)$$

which follows from (1.10). Using the arguments in Appendix A (see Eq. (A.2) especially), we easily see that the CL (1.8) has another continuous solution

$$u(t, x) = \pi - U(x) + V(t), \quad (4.3)$$

where the constant  $C$  also satisfies (4.2).

**Proposition 4.1.** *Let  $pK/a < 2/\pi$ . The two continuous solutions (4.1) and (4.3) exist in the CL (1.8) if*

$$b_1 \geq \frac{1}{2}a - \frac{1}{4}\pi pK. \quad (4.4)$$

*Proof.* We only have to show that Eq. (4.2) has a solution if  $pK/a < 2/\pi$ . Letting

$$\varphi(\eta) = \frac{\beta_0 - \left(\arcsin \eta + \eta \sqrt{1 - \eta^2}\right)}{\eta}, \quad \beta_0 = \frac{a}{pK},$$

we rewrite (4.2) as

$$b_1 = \frac{1}{2}pK \varphi\left(\frac{a}{2(pKC + b_1)}\right).$$

Since  $\varphi(\eta)$  is monotonically decreasing on  $(0, 1)$  and

$$\lim_{\eta \rightarrow 0} \varphi(\eta) = +\infty, \quad \varphi(1) = \beta_0 - \frac{1}{2}\pi,$$

we see that Eq. (4.2) has a solution  $C > 0$  if

$$b_1 \geq \frac{1}{2}pK \left( \beta_0 - \frac{1}{2}\pi \right),$$

which yields (4.4). This implies the desired result.  $\square$

**Remark 4.2.** *As shown in Section 7 of [40], if  $pK/a < 2/\pi$ , then such continuous solutions as (4.1) and (4.3) does not exist in the CL (1.8) with  $b_1, b_0 = 0$ , i.e., in the CL (1.5).*

Let  $m_{\pm}$  be nonnegative integers that may be infinite, and let  $\hat{I}_j^{\pm} \subset [0, 1]$ ,  $j \in [m_{\pm}]$ , be intervals such that  $\hat{I}_j^- \in [0, \frac{1}{2}]$ ,  $\hat{I}_j^+ \in [\frac{1}{2}, 1]$ ,  $\hat{I}_j^- \cap \hat{I}_k^- = \emptyset$ ,  $\hat{I}_j^+ \cap \hat{I}_k^+ = \emptyset$  and

$$\hat{I} = \bigcup_{j=1}^{m_-} \hat{I}_j^- \cup \bigcup_{j=1}^{m_+} \hat{I}_j^+ \neq \emptyset,$$

where the interiors of  $\hat{I}_j^{\pm}$ ,  $j \in [m_{\pm}]$ , may be empty. The CL (1.8) has discontinuous solutions

$$u(t, x) = \begin{cases} U(x) + V(t) & \text{for } x \in [0, 1] \setminus \hat{I}; \\ \pi - U(x) + V(t) & \text{for } x \in \hat{I}_j^+, j \in [m_+]; \\ -U(x) - \pi + V(t) & \text{for } x \in \hat{I}_j^-, j \in [m_-], \end{cases} \quad (4.5)$$

where the constant  $C$  in  $U(x)$  satisfies

$$C = \int_{[0,1] \setminus \hat{I}} \sqrt{1 - \left( \frac{a(x - \frac{1}{2})}{pKC + b_1} \right)^2} dx - \int_{\hat{I}} \sqrt{1 - \left( \frac{a(x - \frac{1}{2})}{pKC + b_1} \right)^2} dx.$$

We see that the synchronized solution given by (3.3) converges to (4.5) as  $n \rightarrow \infty$  when

$$\sigma_i = \begin{cases} 1 & \text{if } i/n \in [0, 1] \setminus \hat{I}; \\ -1 & \text{if } i/n \in \hat{I}. \end{cases} \quad (4.6)$$

Using Theorems 2.3 and 2.6, we prove the following

**Theorem 4.3.** *Let  $pK/a < 2/\pi$  and  $b_1 > 0$ . Then the following hold:*

- (i) *The continuous solution (4.1) is asymptotically stable while the continuous solution (4.3) is unstable when condition (4.4) holds;*
- (ii) *The discontinuous solution (4.5) with  $\hat{I} \neq \emptyset$  is unstable if it exists and is different from (4.1) in the sense of  $L^2(I)$ .*

*Proof.* The synchronized solution (3.19) with  $\sigma_i = 1$  (resp.  $\sigma_i = -1$ ),  $i \in [n]$ , which is asymptotically stable for  $\xi < \xi_0$  (resp. unstable for  $\xi \in (0, 1)$ ) in the CKM (1.7) by Theorem 3.10(i), converges to the continuous solution (4.1) (resp. (4.3)) as  $n \rightarrow \infty$ . Recall that  $\bar{\chi}^{\sigma}(\xi)$  has a unique extremum (local maximum) at  $\xi = \xi_0$  (see Theorem 3.6(i)).

Let  $\sigma_i = 1$ ,  $i \in [n]$ . Since

$$\chi^{\sigma}(\xi) \rightarrow 2 \int_0^1 \sqrt{1 - \xi^2 x^2} dx = \frac{\xi \sqrt{1 - \xi^2} + \arcsin \xi}{2\xi},$$

we have

$$\bar{\chi}^\sigma(\xi) = \frac{\xi}{\beta - \xi\chi^\sigma(\xi)} \rightarrow \frac{2\xi}{2\beta - (\xi\sqrt{1-\xi^2} + \arcsin\xi)} =: \bar{\chi}_0(\xi).$$

Noting that

$$\frac{d}{d\xi} \left( \xi\sqrt{1-\xi^2} + \arcsin\xi \right) = 2\sqrt{1-\xi^2} > 0,$$

we see that  $\bar{\chi}_0(\xi)$  is monotonically increasing on  $(0, 1)$ . This implies that  $\xi_0 \rightarrow 1$  as  $n \rightarrow \infty$ . Using Theorem 2.3(i), we obtain part (i).

We turn to the proof of part (ii). The synchronized solution (3.19) with (4.6), which is unstable by Theorem 3.10(ii), converges to the discontinuous solution (4.5) in  $L^2(I)$  as  $n \rightarrow \infty$ . Hence, by Theorem 2.6, if it is different from (4.1) in the sense of  $L^2(I)$ , then the discontinuous solution (4.5) with  $\hat{I} \neq \emptyset$  is unstable.  $\square$

**Remark 4.4.** *From the proof of Theorem 4.3 we see that condition (3.9) becomes (4.4) as  $n \rightarrow \infty$ .*

From Theorems 3.6 and 3.10 we obtain the following results for the CKM (1.7) on complete graphs:

- The synchronized solution (3.3) for  $v^\sigma$  with  $\sigma_i = 1$ ,  $i \in [n]$ , suffers a saddle-node bifurcation at  $\xi = \xi_0$ , i.e.,  $b_1 = pK/\bar{\chi}^\sigma(\xi_0)$ , and it turns unstable from stable there.
- In addition, it suffers a pitchfork bifurcation at  $\xi = 1$ , i.e.,  $b_1 = pK/\bar{\chi}^\sigma(1)$ , where it changes to a synchronized solution with  $\sigma_1 = \sigma_n = -1$  and  $\sigma_j = 1$ ,  $j \in [n-1] \setminus \{1\}$ , while the two synchronized solutions with  $\sigma_1 = -1$ ,  $\sigma_n = 1$  or  $\sigma_1 = 1$ ,  $\sigma_n = -1$  and  $\sigma_j = 1$ ,  $j \in [n-1] \setminus \{1\}$ , are born.

When  $n \rightarrow \infty$ , the saddle-node and pitchfork bifurcations collide, since  $\xi_0 \rightarrow 1$  as shown in the proof of Theorem 4.3. By Theorem 4.3, these four solutions converge to a single asymptotically stable solution in the sense of  $L^2(I)$  in the CL (1.8). More generally, if  $\sigma_i = 1$  except for a fixed finite positive number of  $i \in [n]$ , then by Theorem 4.3(ii) the synchronized solution (3.3) for  $v^\sigma$  is unstable but converges to the asymptotically stable solution (4.1) in  $L^2(I)$  as  $n \rightarrow \infty$ . Thus, bifurcation behavior in the CL (1.8) is very subtle, compared with such finite-dimensional dynamical systems as the CKM (1.7). Such behavior was previously detected for the KM (1.1) on complete simple graphs in [40].

## 5. CONTROLLED KURAMOTO MODEL ON UNIFORM RANDOM GRAPHS

We turn to the CKM (1.7) with the natural frequencies (1.18) on uniform random dense and sparse graphs given by (1.2) and (1.3), respectively. In contrast to the case of complete graphs, the randomness of the coupling makes a direct analytical characterization of equilibria and their stability in the CKM (1.7) highly difficult. However, the relationships between the CKM (1.7) and CL (1.8) stated in Section 2 allow us to describe fundamental dynamical behavior in the former, by using the results of Section 4 for the latter.

Let  $\bar{\mathbf{u}}(t)$  (resp.  $\hat{\mathbf{u}}(t)$ ) denote solutions (4.1) (resp. (4.3) or (4.5)) to the CL (1.8), such that  $\bar{\mathbf{u}}(t)$  and  $\hat{\mathbf{u}}(t)$  are different in  $L^2(I)$ . Using Corollary 2.5 and Theorems 2.7 and 4.3, we prove the following.

**Theorem 5.1.**

- (i) For any  $\varepsilon, \tau > 0$  there exists  $\delta, N > 0$  such that for any  $n > N$  if  $\mathbf{u}_n(t)$  is any solution to the CKM (1.7) satisfying

$$\|\mathbf{u}_n(0) - \bar{\mathbf{u}}(0)\| < \delta,$$

then

$$\max_{t \in [0, \tau]} \|\mathbf{u}_n(t) - \bar{\mathbf{u}}(t)\| < \varepsilon \quad a.s.$$

Moreover,

$$\lim_{t \rightarrow \infty} \lim_{n \rightarrow \infty} \|\mathbf{u}_n(t) - \bar{\mathbf{u}}(t)\| = 0 \quad a.s.$$

- (ii) Let For any  $\varepsilon, \delta > 0$  there exist  $\tau, N > 0$  such that for  $n > N$

$$\|\mathbf{u}_n(\tau) - \hat{\mathbf{u}}(\tau)\| > \varepsilon \quad a.s.,$$

where  $\mathbf{u}_n(t)$  denote a solution to the KM (1.7) satisfying

$$\|\mathbf{u}_n(0) - \bar{\mathbf{u}}(0)\| < \delta.$$

*Proof.* By Theorem 4.3,  $\bar{\mathbf{u}}(t)$  and  $\hat{\mathbf{u}}(t)$  are, respectively, asymptotically stable and unstable solutions in the CL (1.8). Hence, parts (i) and (ii) immediately follow from Corollary 2.5 and Theorem 2.7, respectively.  $\square$

**Remark 5.2.** For Kuramoto-type models on complete simple or general graphs, mean-field limits have been extensively studied, leading to kinetic equations for the probability density of oscillator phases [1, 3–5]. These approaches describe the evolution of phase distributions rather than the time histories of individual phases, which are random processes when the natural frequencies or the underlying graph  $G_n$  is random. Moreover, in many concrete mean-field analyses such as [3–5], the natural frequencies are modeled as random variables with a prescribed probability distribution, typically satisfying a unimodality assumption.

In contrast, we consider deterministic, uniformly spaced natural frequencies, for which synchronized solutions of the CKM (1.7) and their bifurcations can be analyzed directly. The CL (1.8) adopted here describes the almost sure convergence of solutions of the CKM (1.7) to those of (1.8) as  $n \rightarrow \infty$ . From the mean-field perspective, such limiting states correspond to singular measures, typically delta distributions, and capturing their stability and bifurcation structure within the kinetic framework is highly nontrivial.

Thus, the solution (4.1) behaves (resp. the solutions (4.3) and (4.5) behave) as if it is an asymptotically stable one (resp. they are unstable ones) in the CKM (1.7) on uniform random dense and sparse graphs. Similar behavior was previously numerically observed or theoretically detected for the KMs defined on some random dense and sparse graphs and their CLs including the KM (1.1) and CL (1.5) when the natural frequencies are deterministic or random, in [19, 41–44].

## 6. NUMERICAL SIMULATIONS

We finally present numerical simulation results for the CKM (1.7). We treat the following three cases for the graph  $G_n$ :

- (i) Complete simple graph, which is deterministic dense with  $p = 1$ ;
- (ii) Random undirected dense graph in which  $w_{ij}^n = 1$  with probability

$$\mathbb{P}(i \sim j) = p, \quad i, j \in [n]; \quad (6.1)$$

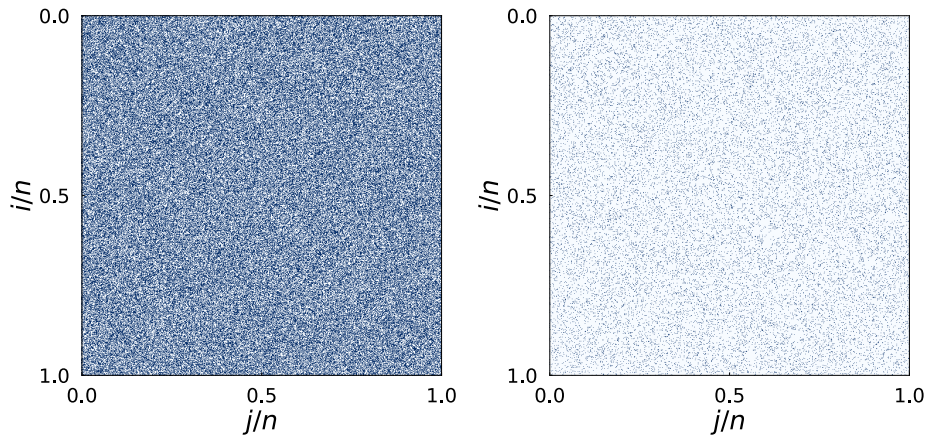


FIGURE 3. Pixel pictures of sampled weighted matrices for the random undirected graphs given by  $w_{ij}^n = 1$ ,  $i, j \in [n]$  with probability (6.1) and (6.2) for  $n = 1000$ : (a) Dense graph with  $p = 0.5$ ; (b) Sparse graph with  $p = 0.5$  and  $\gamma = 0.3$ . The color of the corresponding pixel is blue if  $w_{ij} = 1$  and it is light blue otherwise.

(iii) Random undirected sparse graph in which  $w_{ij}^n = 1$  with probability

$$\mathbb{P}(i \sim j) = n^{-\gamma}p, \quad i, j \in [n], \quad (6.2)$$

where  $\gamma \in (0, \frac{1}{2})$ . Recall that  $\alpha_n = n^{-\gamma}$  and note that  $\alpha_n^{-1} = n^\gamma > 1$  for any  $n > 1$ .

We specifically take  $p = 0.5$  in case (ii) and  $p = 0.5$  and  $\gamma = 0.3$  in case (iii). Figures 3(a) and (b) provide numerically computed samples of the weight matrices for the random undirected dense and sparse graphs in cases (ii) and (iii), respectively, with  $n = 1000$ ,  $p = 0.5$  and  $\gamma = 0.3$ .

We carried out numerical simulations for the CKM (1.7) on the three types of graphs with  $n = 1000$ ,  $V_1 = b_0 = 1$  and  $V_0 = 1$  using the DOP853 solver [17]. We also chose  $K = 0.5$  and  $a = 1$  for case (i), and  $K = 0.5$  and  $a = 0.5$  for cases (ii) and (iii). The continuous solution (4.1) does not exist in the CL (1.8) with  $b_1, b_0 = 0$ , in cases (i)-(iii) since  $pK/a = 0.5 < 2/\pi = 0.63661\dots$  (see Remark 4.2). The initial values  $u_i^n(0)$ ,  $i \in [n]$  were independently randomly chosen according to the uniform distribution on  $[-\pi, \pi]$ .

Figures 4(a), (b) and (c) show the time-histories of every 100th node (from 50th to 950th) in cases (i), (ii) and (iii), respectively, for  $b_1 = 0.2$ , in which the asymptotically stable solution (4.1) exists in the CL (1.8). The ordinates represent the deviations of the responses from the desired motion,  $u_i^n(t) - V(t)$ . We observe that the responses rapidly converge to the synchronized solution around the desired motion, as predicted theoretically in Sections 3 and 5.

In Figs. 5(a), (b) and (c), the deviations of the responses from the desired motion at time  $t = 100$ , which may be regarded as the steady states from Fig. 4, are plotted for cases (i), (ii) and (iii), respectively. Here the same initial condition and value of  $b_1$  as in Fig. 4 were used. The blue line in each figure represents the corresponding theoretical predictions computed from the synchronized solution (4.1) in the CL

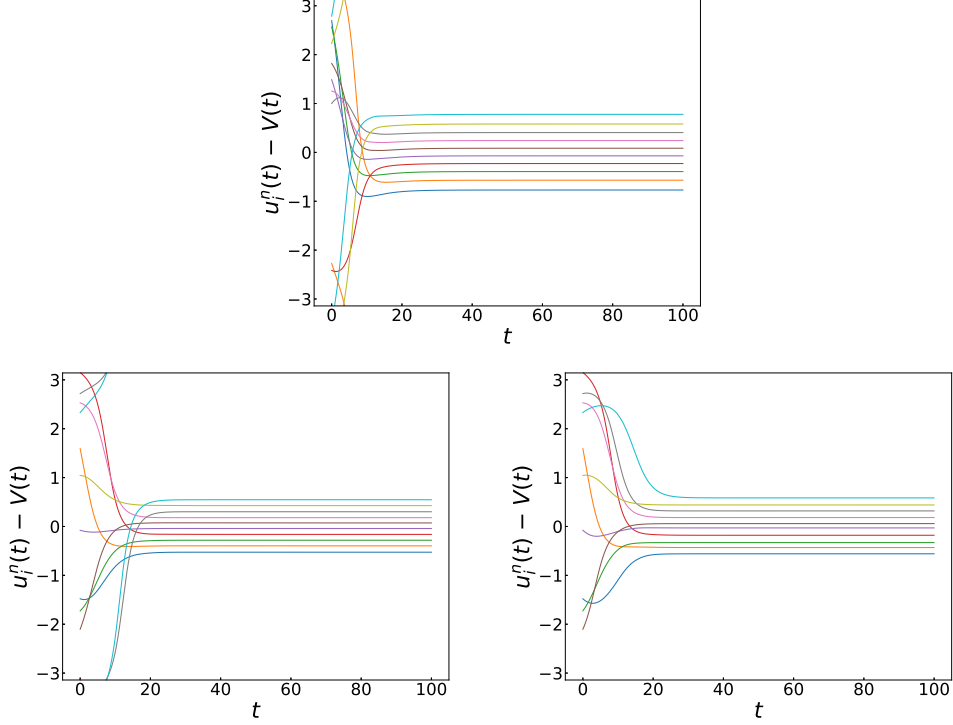


FIGURE 4. Numerical simulation results of the CKM (1.7) with  $n = 1000$ ,  $K = 0.5$ ,  $V_1, b_0 = 1$ ,  $V_0 = 1$  and  $b_1 = 0.2$ : (a)  $(a, p) = (1, 1)$  in case (i); (b)  $(0.5, 0.5)$  in case (ii); (c)  $(a, p, \gamma) = (0.5, 0.5, 0.3)$  in case (iii). The time-history of every 100th node (from 50th to 950th) is plotted with different colors.

(1.8). The agreement between the numerical results and theoretical predictions is excellent for cases (i) and (ii) in Fig. 5(a) and (b), and good for case (iii) in Fig. 5(c) although some fluctuations due to randomness are found in the latter. Thus, we observe that the synchronized solution (4.1) behaves as it is an asymptotically stable one in the CKM (1.7).

Figures 6(a), (b) and (c) display the maximal and minimal deviations of the steady-state responses from the desired motion in cases (i), (ii) and (iii), respectively, when the feedback gain  $b_1$  is varied. The blue line in each figure represents the corresponding theoretical predictions  $\pm\Delta u$  with

$$\Delta u = \arcsin\left(\frac{a}{2(pKC + b_1)}\right) \quad (6.3)$$

computed from the synchronized solution (4.1) in the CL (1.8), where  $C$  satisfies (4.2), and the green line represents the critical value of  $b_1$  given by (4.4) at which the solution suddenly appears when  $b_1$  is increased. We observe that the steady-state responses tend to the desired motion as  $b_1 \rightarrow \infty$ . The agreement between the numerical results and theoretical predictions is excellent for cases (i) and (ii) in Fig. 6(a) and (b), and good for case (iii) in Fig. 6(c), again.

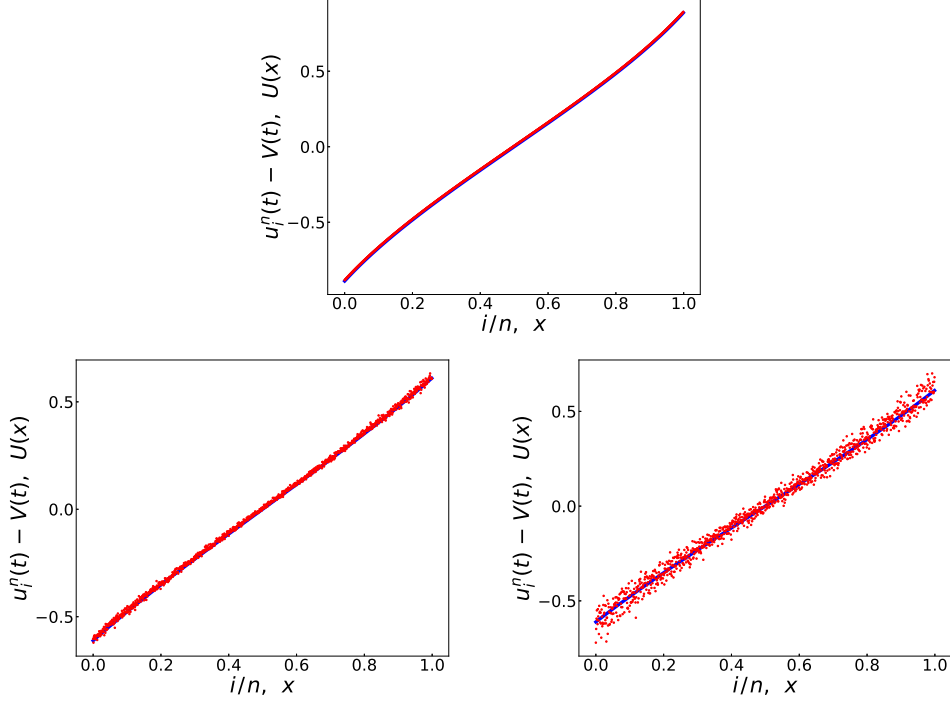


FIGURE 5. Deviations of steady-state responses from the desired motion in the CKM (1.7) with  $n = 1000$ ,  $K = 0.5$ ,  $V_1, b_0 = 1$ ,  $V_0 = 1$  and  $b_1 = 0.2$ : (a)  $(a, p) = (1, 1)$  in case (i); (b)  $(0.5, 0.5)$  in case (ii); (c)  $(a, p, \gamma) = (0.5, 0.5, 0.3)$  in case (iii). Here  $u_i^n(t) - V(t)$ ,  $i \in [n]$ , with  $t = 100$  are plotted as red dots. The blue line represents the corresponding theoretical predictions computed from the synchronized solution (4.1) in the CL (1.8).

#### ACKNOWLEDGMENTS

This work was partially supported by JSPS KAKENHI Grant Number JP23K22409. The author thanks Dongeon Kim for his assistance in numerical computations.

#### APPENDIX A. DERIVATION OF (1.9) AND (1.13)

We first derive the solution (1.9) to the CL (1.8). We substitute  $u(t, x) = \tilde{U}(x) + V(t)$  into (1.8) to obtain

$$\begin{aligned} V_1 &= \omega(x) + pK \cos \tilde{U}(x) \int_I \sin \tilde{U}(y) dy \\ &\quad - pK \sin \tilde{U}(x) \int_I \cos \tilde{U}(y) dy - b_1 \sin \tilde{U}(x) + b_0 \\ &= \omega(x) - \tilde{C} \sin(\tilde{U}(x) - \psi) + b_0, \end{aligned}$$

where

$$\tilde{C} \cos \psi = pK \int_I \cos \tilde{U}(y) dy + b_1, \quad \tilde{C} \sin \psi = pK \int_I \sin \tilde{U}(y) dy. \quad (\text{A.1})$$

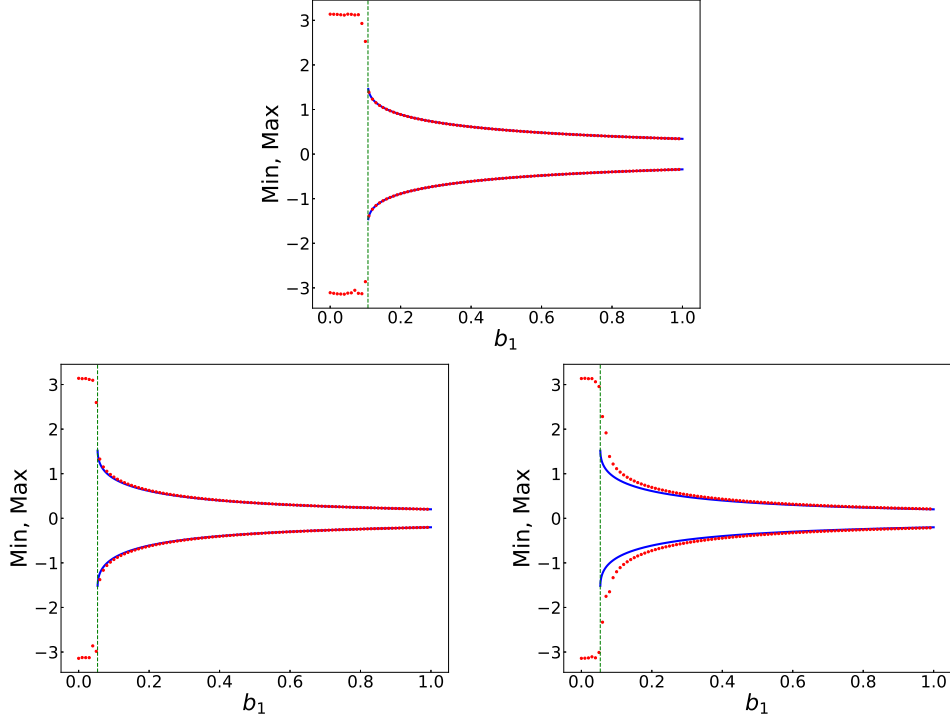


FIGURE 6. Maximal and minimal deviations of the steady-state responses from the desired motion in the CKM (1.7) with  $n = 1000$ ,  $K = 0.5$ ,  $V_1, b_0 = 1$  and  $V_0 = 1$  when the feedback gain  $b_1$  is changed: (a)  $(a, p) = (1, 1)$  in case (i); (b)  $(0.5, 0.5)$  in case (ii); (c)  $(a, p, \gamma) = (0.5, 0.5, 0.3)$  in case (iii). Here  $\max_{i \in [n]}(u_i^n(t) - V(t))$  and  $\min_{i \in [n]}(u_i^n(t) - V(t))$ ,  $i \in [n]$ , for  $t > 0$  sufficiently large are plotted as red dots. The blue line represents the corresponding theoretical predictions  $\pm \Delta u$  computed from the synchronized solution (4.1) in the CL (1.8), where  $\Delta u$  is given by (6.3).

Obviously,  $\tilde{C} \neq 0$  since  $\omega(x) - V_1 + b_0 \equiv 0$  otherwise. Hence, we have

$$\sin(\tilde{U}(x) - \psi) = \frac{\omega(x) - V_1 + b_0}{\tilde{C}}, \quad (\text{A.2})$$

which yields

$$\tilde{U}(x) = \arcsin\left(\frac{\omega(x) - V_1 + b_0}{\tilde{C}}\right) + \psi \quad (\text{A.3})$$

and

$$\begin{aligned} \tilde{C} \cos \psi &= pK \cos \psi \int_I \sqrt{1 - \left(\frac{\omega(y) - V_1 + b_0}{\tilde{C}}\right)^2} dy + b_1, \\ \tilde{C} \sin \psi &= pK \sin \psi \int_I \sqrt{1 - \left(\frac{\omega(y) - V_1 + b_0}{\tilde{C}}\right)^2} dy \end{aligned} \quad (\text{A.4})$$

by (A.1) since by (1.11)

$$\int_I (\omega(y) - V_1 + b_0) dy = 0.$$

From (A.4) we obtain  $\psi = 0$  and

$$\tilde{C} = pK \int_I \sqrt{1 - \left( \frac{\omega(y) - V_1 + b_0}{\tilde{C}} \right)^2} dy + b_1. \quad (\text{A.5})$$

Comparing (A.5) with (1.10), we see that  $\tilde{C} = pKC + b_1$ , so that  $\tilde{U}(x) = U(x)$  by (A.3). Thus, we obtain the solution (1.9).

We next derive the solution (1.13) to the CKM (1.7) with  $w_{ij}^n = p$ ,  $i, j \in [n]$ , and  $\alpha_n = 1$ . We substitute  $u_i^n(t) = \tilde{U}_i^n + V(t)$  into (1.7) to obtain

$$\begin{aligned} V_1 &= \omega_i^n + \frac{pK}{n} \cos \tilde{U}_i^n \sum_{j=1}^n \sin \tilde{U}_j^n - \frac{pK}{n} \sin \tilde{U}_i^n \sum_{j=1}^n \cos \tilde{U}_j^n - b_1 \sin \tilde{U}_i^n + b_0 \\ &= \omega_i^n - \tilde{C}_D \sin(\tilde{U}_i^n - \psi) + b_0 \end{aligned}$$

where

$$\tilde{C}_D \cos \psi = \frac{pK}{n} \sum_{j=1}^n \cos \tilde{U}_j^n + b_1, \quad \tilde{C}_D \sin \psi = \frac{pK}{n} \sum_{j=1}^n \sin \tilde{U}_j^n. \quad (\text{A.6})$$

Hence, we have

$$\tilde{U}_i^n = \arcsin \left( \frac{\omega_i^n - V_1 + b_0}{\tilde{C}_D} \right) + \psi, \quad i \in [n], \quad (\text{A.7})$$

and

$$\begin{aligned} \tilde{C}_D \cos \psi &= \frac{pK}{n} \cos \psi \sum_{j=1}^n \sqrt{1 - \left( \frac{\omega_j^n - V_1 + b_0}{\tilde{C}_D} \right)^2} + b_1, \\ \tilde{C}_D \sin \psi &= \frac{pK}{n} \sin \psi \sum_{j=1}^n \sqrt{1 - \left( \frac{\omega_j^n - V_1 + b_0}{\tilde{C}_D} \right)^2} \end{aligned} \quad (\text{A.8})$$

by (A.6) since by (1.16)

$$\frac{1}{n} \sum_{j=1}^n \omega_j^n - V_1 + b_0 = 0.$$

From (A.8) we obtain  $\psi = 0$  and

$$\tilde{C}_D = \frac{pK}{n} \sum_{j=1}^n \sqrt{1 - \left( \frac{\omega_j^n - V_1 + b_0}{\tilde{C}_D} \right)^2} + b_1. \quad (\text{A.9})$$

Comparing (A.9) with (1.14), we see that  $\tilde{C}_D = pKC_D + b_1$ , so that  $\tilde{U}_i^n = U_i^n$ ,  $i \in [n]$ , by (A.7). Thus, we obtain the solution (1.13).

## REFERENCES

- [1] J.A. Acebrón, L.L. Bonilla, C.J.P. Vicente, F. Ritort and R. Spigler, The Kuramoto model: A simple paradigm for synchronization phenomena, *Rev. Mod. Phys.*, **77** (2005), 137–185.
- [2] A. Arenas, A. Diaz-Guilera, J. Kurths, Y. Moreno and C. Zhou, Synchronization in complex networks, *Phys. Rep.*, **469**(2008), 93–153.
- [3] H. Chiba, A proof of the Kuramoto conjecture for a bifurcation structure of the infinite-dimensional Kuramoto model, *Ergodic Theory Dynam. Systems*, **35** (2015), 762–834.
- [4] H. Chiba and G.S. Medvedev, The mean field analysis of the Kuramoto model on graphs I: The mean field equation and transition point formulas, *Discrete Contin. Dyn. Syst.*, **39** (2019a), 131–155.
- [5] H. Chiba and G.S. Medvedev, The mean field analysis of the Kuramoto model on graphs II: Asymptotic stability of the incoherent state, center manifold reduction, and bifurcations, *Discrete Contin. Dyn. Syst.*, **39** (2019), 3897–3921.
- [6] S.P. Cornelius, W.L. Kath and A.E. Motter, Realistic control of network dynamics, *Nat. Commun.*, **4** (2013), 1942.
- [7] E.A. Coddington and N. Levinson, *Theory of Ordinary Differential Equations*, McGraw-Hill, New York, 1955.
- [8] R. Delabays, O. Jacquod and F. Dörfler, The Kuramoto model on oriented and signed graphs, *SIAM J. Appl. Dyn. Syst.*, **18** (2019), 458–480.
- [9] F. Dörfler and F. Bullo, Synchronization in complex networks of phase oscillators: A survey, *Automatica*, **50** (2014), 1539–1564.
- [10] C. Duan, T. Nishikawa and A.E. Motter, Prevalence and scalable control of localized networks, *Proc. Natl. Acad. Sci. USA*, **119** (2022), e2122566119.t
- [11] G.B. Ermentrout, Synchronization in a pool of mutually coupled oscillators with random frequencies, *J. Math. Biol.*, **22** (1985), 1–9.
- [12] S. Gao and P.E. Caines, Graphon control of large-scale networks of linear systems, *IEEE Trans. Automat. Contr.*, **65** (2020), 4090–4105.
- [13] S. Gao and P.E. Caines, Subspace decomposition for graphon LQR: Applications to VLSNs of harmonic oscillators, *IEEE Trans. Control. Netw. Syst.*, **8** (2021), 576–586.
- [14] T. Girnyk, M. Hasler and Y. Maistrenko, Multistability of twisted states in non-locally coupled Kuramoto-type models, *Chaos*, **22** (2012), 013114.
- [15] J. Guckenheimer and P. Holmes, *Nonlinear Oscillations, Dynamical Systems, and Bifurcations of Vector Fields*, Springer, New York, 1983.
- [16] S.-Y. Ha, H.K. Kim and S.W. Ryoo, Emergence of phase-locked states for the Kuramoto model in a large coupling regime, *Commun. Math. Sci.*, **14** (2016), 1073–1091.
- [17] E. Hairer, S.P. Nørsett and G. Wanner, *Solving Ordinary Differential Equations I: Nonstiff Problems*, 2nd ed. Springer, Berlin, 1993.
- [18] M. Haragus and G. Iooss, *Local Bifurcations, Center Manifolds, and Normal Forms in Infinite-Dimensional Dynamical Systems*, Springer, London, 2011.
- [19] R. Ihara and K. Yagasaki, Continuum limits of coupled oscillator networks depending on multiple sparse graphs, *J. Nonlinear Sci.*, **33** (2023), 62; Correction, **35** (2025), 27.
- [20] D. Kaliuzhnyi-Verbovetskyi and G. S. Medvedev, The semilinear heat equation on sparse random graphs, *SIAM J. Math. Anal.*, **49** (2017), no. 2, 1333–1355.
- [21] D. Kim and K. Yagasaki, Feedback control of the Kuramoto model defined on graphs II: Rational natural frequencies, in preparation.
- [22] Y. Kuramoto, Self-entrainment of a population of coupled non-linear oscillators, in *International Symposium on Mathematical Problems in Theoretical Physics*, H. Araki (ed.), Springer, Berlin, 1975, pp. 420–422.
- [23] Y. Kuramoto, *Chemical Oscillations, Waves, and Turbulence*, Springer, Berlin, 1984.
- [24] Y.A. Kuznetsov, *Elements of Applied Bifurcation Theory*, Springer, New York, 2004.
- [25] X. Li and P. Rao, Synchronizing a weighted and weakly-connected Kuramoto-oscillator digraph with a pacemaker, *IEEE Trans. Circuits Syst. I: Reg. Papers*, **62** (2017), 899–905.
- [26] L. Lovász, *Large Networks and Graph Limits*, AMS, Providence RI, 2012.
- [27] G.S. Medvedev, The nonlinear heat equation on dense graphs and graph limits, *SIAM J. Math. Anal.*, **46** (2014), 2743–2766.
- [28] G.S. Medvedev, The nonlinear heat equation on W-random graphs, *Arch. Ration. Mech. Anal.*, **212** (2014), 781–803.

- [29] G.S. Medvedev, Small-world networks of Kuramoto oscillators, *Phys. D*, **266** (2014), 13–22.
- [30] G.S. Medvedev, The continuum limit of the Kuramoto model on sparse random graphs, *Comm. Math. Sci.*, **17** (2019), no. 4, 883–898.
- [31] G.S. Medvedev and J.D. Wright, Stability of twisted states in the continuum Kuramoto model, *SIAM J. Appl. Dyn. Syst.*, **16** (2017), 188–203.
- [32] A.E. Motter, Networkcontrology, *Chaos*, **25** (2015), 097621.
- [33] A. Pikovsky and M. Rosenblum, Dynamics of globally coupled oscillators: Progress and perspectives, *Chaos*, **25** (2015), 097616.
- [34] A. Pikovsky, M. Rosenblum, and J. Kurths, *Synchronization: A Universal Concept in Non-linear Sciences*, Cambridge University Press, Cambridge, 2001.
- [35] F.A. Rodrigues, T.K.D.M. Peron, P. Ji and J. Kurths, The Kuramoto model in complex networks, *Phys. Rep.*, **610** (2016), 1–98.
- [36] P. S. Skardal and A. Arenas, Control of coupled oscillator networks with application to microgrid technologies, *Science Advances*, **1** (2015), e1500339.
- [37] S.H. Strogatz, From Kuramoto to Crawford: Exploring the onset of synchronization in populations of coupled oscillators, *Phys. D*, **143** (2000), 1–20.
- [38] S. Wiggins, *Introduction to Applied Nonlinear Dynamical Systems and Chaos*, Springer, New York, 2003.
- [39] D.A. Wiley, S.H. Strogatz and M. Girvan, The size of the sync basin, *Chaos*, **16** (2006), 015103.
- [40] K. Yagasaki, Bifurcations and stability of synchronized solutions in the Kuramoto model with uniformly spaced natural frequencies, *Nonlinearity*, **38** (2025), 075032; Corrigendum, **38** (2025), 109501.
- [41] K. Yagasaki, Bifurcations of synchronized solutions in a continuum limit of the Kuramoto model with two-mode interaction depending on two graphs, *SIAM J. Appl. Dyn. Syst.*, **24** (2025), 2345–2368. .
- [42] K. Yagasaki, Bifurcations of twisted solutions in a continuum limit for the Kuramoto model on nearest neighbor graphs, *J. Nonlinear Sci.*, in press.
- [43] K. Yagasaki, Feedback control of twisted states in the Kuramoto model on nearest neighbor and complete simple graphs, submitted for publication.
- [44] K. Yagasaki, Continuum limit of the Kuramoto model with random natural frequencies on uniform graphs, *Phys. D*, **481** (2025), 134818.
- [45] J. Wu and X. Li, Collective synchronization of Kuramoto-oscillator networks, *IEEE Circuits Syst. Mag.*, **20** (2020), 46–67.

DEPARTMENT OF APPLIED MATHEMATICS AND PHYSICS, GRADUATE SCHOOL OF INFORMATICS,  
 KYOTO UNIVERSITY, YOSHIDA-HONMACHI, SAKYO-KU, KYOTO 606-8501, JAPAN  
*Email address:* yagasaki@amp.i.kyoto-u.ac.jp